JOURNAL OF
Materials
CHEMISTRY

Synthesis, crystal structure and thermal behaviour of $CdZrK_2(C_2O_4)_4 \cdot 8H_2O$

Erwann Jeanneau, Nathalie Audebrand and Daniel Louër*

Laboratoire de Chimie du Solide et Inorganique Moléculaire, UMR CNRS 6511, Institut de Chimie, Université de Rennes I, Avenue du Général Leclerc, 35042 Rennes cedex, France.
E-mail: Daniel.Louer@univ-rennes1.fr

Received 8th March 2002, Accepted 22nd May 2002
First published as an Advance Article on the web 28th June 2002

The crystal structure of the new ternary oxalate $CdZrK_2(C_2O_4)_4 \cdot 8H_2O$ was solved from single-crystal diffraction data. The crystal data are as follows: tetragonal symmetry, space group $I\bar{4}$ (No. 82), $a = 11.216(5)$, $c = 8.954(5)$ Å, $Z = 2$. The structure is built from 8-fold coordinated cadmium, zirconium and potassium atoms. It consists of zigzag chains formed by alternated CdO_8 and ZrO_8 polyhedra connected by bidentate oxalate groups. The chains are linked together through KO_8 polyhedra. Relationships with the structure of cadmium zirconium oxalate is discussed, as well as the various structure types already known. It is shown that the crystal structures are characterised by chemically identical $[CdZr(C_2O_4)_4]^{2-}$ anionic frameworks with different topologies, in which the additional cations are inserted. This structure overview suggests the possibility of conceiving new cadmium–zirconium–oxalate based materials. The thermal behaviour of the new compound is described in detail from temperature dependent X-ray powder diffraction and thermogravimetric measurements. The final decomposition product is a mixture of cadmium and zirconium oxides.

Introduction

The synthesis of new compounds with open-framework structures has received considerable attention over the last few years (see, for example, refs. 1–3). In particular, many oxalate-based compounds with microporous structure frameworks have been reported.[2,4,5] This topology is responsible for 'zeolitic' properties due to weakly bonded water molecules, which were thoroughly investigated in recent studies.[5,6] Another interesting property of mixed metal oxalates is their low thermal stability allowing the preparation of nanocrystalline mixed oxides, such as $BaTiO_3$[7] and $PbZrO_3$.[8] In recent studies we have focused our attention on mixed oxalate compounds formed from metals having an eight-fold coordination, such as $YK(C_2O_4)_2 \cdot 4H_2O$,[5] $Pb_2Zr(C_2O_4)_4 \cdot nH_2O$,[8] $Cd_2Zr(C_2O_4)_4 \cdot 6H_2O$,[6] $CdZr(NH_4)_2(C_2O_4)_4 \cdot 4H_2O$ and $CdZr(C_2N_2H_{10})(C_2O_4)_4 \cdot 4H_2O$.[9] Although cadmium atoms are generally six-fold coordinated, eight-fold coordination has been found in a few compounds,[6,9–11] and is also present in the listed cadmium zirconium phases together with eight-fold coordinated zirconium atoms.[6,9] Additionally, there are two frequent configurations which dominate the stereochemistry of eight-fold coordination, *i.e.* the dodecahedral and the square antiprismatic configurations.[12] The two configurations have been reported for the polyhedra CdO_8 and ZrO_8 in the structures of the cadmium zirconium compounds, leading to a high flexibility for the formation of varied phases in the family, *e.g.* dodecahedra are found in $Cd_2Zr(C_2O_4)_4 \cdot 6H_2O$[6] while square antiprisms have been reported in $CdZr(NH_4)_2(C_2O_4)_4 \cdot 4H_2O$ and $CdZr(C_2N_2H_{10})(C_2O_4)_4 \cdot 4H_2O$.[9] This combined feature of eight-coordination with two stereochemical configurations, in which oxalate groups can span particular edges, constitutes an interesting parameter for expecting new structural arrangements in the family. This is demonstrated here with the study of a new ternary oxalate compound based on cadmium, zirconium and potassium elements. The crystal structure determination and the thermal behaviour of this phase are reported and the crystal chemistry of the cadmium zirconium family is discussed.

Synthesis

Crystals of cadmium zirconium potassium oxalate $CdZrK_2(C_2O_4)_4 \cdot 8H_2O$ were obtained from a soft chemistry route. The compound was synthesised from a mixture of 0.50 g of cadmium nitrate $Cd(NO_3)_2 \cdot 4H_2O$ from Merck and 0.37 g of zirconium oxynitrate $ZrO(NO_3)_2 \cdot xH_2O$ from Alpha [whose correct formula is $Zr(OH)_2(NO_3)_2 \cdot (1 + x)H_2O$][13] in 50 mL of deionized water. This solution was titrated by a 0.1 mol L^{-1} oxalic acid solution in excess until a white precipitate was formed. The mixture was heated up to 80 °C and 2 mL of concentrated KOH was then poured in, still under stirring. Finally, about 4 mL of concentrated HNO_3 was slowly added until complete dissolution. After a few hours, the evaporation of the solution at room temperature led to the formation of bipyramidal-shaped transparent crystals of average size 100 μm. The crystals were then filtered, thoroughly washed with deionized water, ethanol and finally dried under air. The X-ray diffraction pattern of the powdered crystals indicated that the product was a new material. It was subsequently verified that the powder pattern fitted well the simulated one generated from the single crystal structure solution reported in the present study, which demonstrates the purity of the material. The chemical formula was derived from Energy Dispersive X-ray Spectrometry (ratios Cd/Zr/K = 1/1/2), performed by means of a JSM 6400 spectrometer equipped with an Oxford Link Isis analyser and from the crystal structure determination reported below. It is in agreement with the chemical composition $CdZrK_2(C_2O_4)_4 \cdot 8H_2O$. This formula was confirmed by manganimetric titration of the oxalate content in crystals, from which the number 4.025 of oxalate groups per formulae unit was derived. Assuming the above formula, the yield found for this synthesis was 86%. The images made by means of a JEOL JSM-6301 F Scanning Electron Microscope (SEM) showed pseudomorphs of the initial crystals, with cracks due to the sensitivity of the material towards the electron beam (Fig. 1). In addition, from a magnified image, an etching pattern on the surface of the crystals could be observed (Fig. 1), as the probable consequence of the use of concentrated nitric acid in the course of the synthesis.

DOI: 10.1039/b202463m

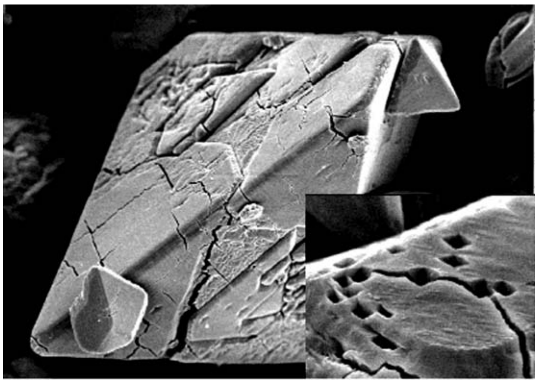

Fig. 1 SEM micrograph displaying bipyramidal shaped pseudomorphs of $CdZrK_2(C_2O_4)_4{\cdot}8H_2O$, with cracks due to the sensitivity of the initial crystals to the electron beam. The close-up on the bottom right shows the typical etching pattern found on the surface of the crystals.

The particular geometry of such etching patterns is generally related to the crystalline structure and surface defects of the product. This is verified in Fig. 1 in which etching images with a square section are clearly observed, according to the tetragonal symmetry of the material. A similar phenomenon was already observed for $CdZr(NH_4)_2(C_2O_4)_4{\cdot}4H_2O$ prepared according to the same synthesis route.[9]

Experimental

Collection of X-ray powder diffraction data

X-Ray powder diffraction data were obtained with a Siemens D500 diffractometer with the parafocusing Bragg–Brentano geometry, using monochromatic Cu Kα_1 radiation (λ = 1.5406 Å) selected with an incident beam curved-crystal germanium monochromator.[14] Additional powder diffraction data were collected *in situ* at different temperatures, with a Bruker AXS D5005 powder diffractometer using a diffracted-beam-graphite monochromator (Cu Kα_1,α_2), equipped with an Anton Paar HTK1200 oven. For pattern indexing, the extraction of the peak positions was carried out with the Socabim program PROFILE, which is a part of the DIFFRACT-AT software package supplied by Bruker AXS. Pattern indexing was performed with the program DICVOL91[15] and full-pattern matching with FULLPROF,[16] available in the software package WinPLOTR.[17]

Temperature-dependent X-ray diffraction (TDXD) was performed under dynamic air with a powder diffractometer combining the curved-position-sensitive (PSD) from INEL (CPS 120) and a high-temperature attachment from Rigaku. The detector was used in a semi-focusing arrangement by reflection (Cu Kα_1 radiation) as described elsewhere.[18]

Single-crystal data collection

A suitable crystal with linear dimensions of about 150 µm was mounted on a four-circle Nonius Kappa CCD diffractometer, using Mo Kα radiation (λ = 0.71073 Å) and equipped with a CCD area detector. The experiment was carried out in the resolution range 20.40–0.62 Å with a crystal-to-detector distance of 25 mm. Intensities were collected by means of the program COLLECT[19] from 182 frames with a step rotation angle of 2° for the ω angle. Each frame was obtained with a total exposure time of 20 seconds. Reflection indexing, Lorentz-polarisation correction, peak integration and background determination were carried out with the program DENZO.[20] Frame scaling and unit-cell parameters refinement were made with the program SCALEPACK,[20] on the basis of 1306 reflections in the θ range 1.00–34.97°. Numerical correction absorption was performed by modelling the crystal faces using NUMABS.[21] The resulting set of *hkl* reflections was used for structure refinement. Crystallographic data and details on data collection are listed in Table 1. Structure drawings were carried out with Diamond 2.1e, supplied by Crystal Impact (Brandenburg, 2001).[22]

CCDC reference number 181534.

See http://www.rsc.org/suppdata/jm/b2/b202463m/ for crystallographic data in CIF or other electronic format.

Table 1 Crystallographic data and structure refinement parameters for $CdZrK_2(C_2O_4)_4{\cdot}8H_2O$

Empirical formula	$CdZrK_2C_8O_{24}H_{16}$
Crystal system	Tetragonal
Space group	$I\bar{4}$ (No. 82)
Crystal size/mm	0.14 × 0.17 × 0.19
a/Å	11.216(5)
c/Å	8.954(5)
V/Å^3	1126.4(9)
Z	2
M/g mol^{-1}	778.03
ρ_{calc}/g cm^{-3}	2.29
λ (Mo Kα)/Å	0.71073
θ range/°	1.02–34.97
Index ranges	$-18 \leqslant h \leqslant 18, -17 \leqslant k \leqslant 18, -14 \leqslant l \leqslant 13$
Unique data	2482
Observed data ($I > 2\sigma(I)$)	2358
R_1 ($I > 2\sigma(I)$)	0.021
R_1 (All)	0.023
wR_2 ($I > 2\sigma(I)$)	0.046
wR_2 (All)	0.047
Refinement method	Full-matrix least-squares on $\lvert F^2 \rvert$
Goodness of fit	1.1
No. of variables	94
No. of restraints	2
Largest difference map peak and hole/e Å^{-3}	0.492 and −0.464

Thermal analysis

Thermogravimetric analyses (TG) were carried out with a Rigaku thermoflex instrument for runs under airflow. The powdered samples were spread evenly in large platinum crucibles to avoid mass effects.

Results

Structure solution

The structure was solved with the tetragonal symmetry in space group $I\bar{4}$. The heavy atoms were located using the direct methods with the program SIR97,[23] while the remaining non-H atoms were found from successive Fourier map analyses with SHELXL97.[24] The hydrogen atoms of the water molecules were found either from Fourier analyses or by means of the CALC-OH[25] program, available in the WINGX software package,[26] and then included in the structure refinement. The last cycles of refinement included atomic positions for all atoms and anisotropic displacement parameters for all non-hydrogen atoms. The H–H distance within the water molecules has been restrained to be equal to 1.3(1) Å so that the H–O–H angles approach the expected theoretical value. The final atomic coordinates are given in Table 2 and selected bond distances and angles in Table 3.

Description of the structure

The three-dimensional structure of $CdZrK_2(C_2O_4)_4{\cdot}8H_2O$ is built from polyhedra of eight-fold coordinated cadmium, zirconium and potassium atoms connected by oxalate groups. The structure can be described by a net of zigzag chains linked

Table 2 Positional and equivalent isotropic atomic displacement parameters with their standard deviations for $CdZrK_2(C_2O_4)_4 \cdot 8H_2O$. $U\mathrm{eq} = (1/3)\sum_i \sum_j U_{ij} a_i^* a_j^* \boldsymbol{a_i} \cdot \boldsymbol{a_j}$

Atom	x	y	z	$U^{\mathrm{eq}}/U_{\mathrm{iso}}/Å^2$
Cd	1/2	1/2	1/2	0.01385(7)
Zr	1/2	0	1/4	0.00993(8)
K1	1/2	1/2	0	0.0240(2)
K2	1/2	0	3/4	0.0274(3)
O1	0.4963(1)	0.8121(1)	0.1891(2)	0.0209(3)
O2	0.4884(1)	0.6219(1)	0.2668(1)	0.0244(3)
O3	0.5018(1)	0.7041(1)	0.5536(1)	0.0231(3)
O4	0.5043(1)	0.8889(1)	0.4583(1)	0.0192(2)
OW1	0.7096(2)	0.6456(2)	0.0423(2)	0.0478(5)
OW2	0.8587(2)	0.7066(2)	0.2921(2)	0.0472(4)
C1	0.4947(1)	0.7294(1)	0.2884(2)	0.0154(3)
C2	0.5004(1)	0.7763(1)	0.4489(2)	0.0155(3)
H11	0.751(2)	0.595(2)	0.991(5)	0.050
H12	0.743(2)	0.654(3)	0.120(3)	0.050
H21	0.828(3)	0.743(2)	0.367(3)	0.050
H22	0.911(2)	0.754(3)	0.249(4)	0.050

to one another through potassium coordination KO_8 polyhedra (Fig. 2). A chain is constituted of alternated CdO_8 and ZrO_8 polyhedra linked through oxalate groups, with Cd–Zr–Cd and Zr–Cd–Zr angles of 136.5°. These chains are running both along the *a* and *b* axes and each cadmium and zirconium coordination polyhedron belongs to two different chains at right angles. These chains contribute to the formation of a three-dimensional framework (Fig. 3), reinforced by in-plane connections through edge-sharing potassium coordination polyhedra. Indeed, as seen in the plane *bc* (Fig. 2) each chain is linked to the adjacent ones through edge-sharing KO_8 polyhedra. The same type of arrangement is observed in the plane *ac*.

The cadmium, zirconium and potassium atoms all adopt the same environment, consisting of eight oxygen atoms forming a dodecahedron, which is, with the square-based antiprism, the most common polyhedron found for eight-fold coordinated atoms. The distances within these dodecahedra are reported in Table 3, using the formalism introduced by Hoard and Silverton.[12] The analysis of the distances with this notation shows that both the zirconium and cadmium environments are close to an ideal D_{2d} dodecahedron, which permits unequal bond lengths M–A and M–B and also edges of four different length, *a* (two), *b* (four), *m* (four) and *g* (eight) (see Fig. 4). The zirconium and cadmium atoms are only surrounded by oxygen atoms from oxalate groups. The average distances in the ZrO_8 and CdO_8 polyhedra are in good agreement with previously reported ones in compounds containing eight-fold coordinated Zr and/or Cd atoms, *e.g.* $Pb_2Zr(C_2O_4)_4 \cdot nH_2O$[8] and $Cd_2Zr(C_2O_4)_4 \cdot 6H_2O$.[6] Furthermore, the mean M–O distances, *i.e.* 2.419(4), 2.211(3), 2.822(2) and 2.864(2) Å for M = Cd, Zr, K1 and K2, respectively, agree well with the theoretical values (2.417, 2.184 and 2.901 Å) calculated with the program VALENCE.[27] The coordination polyhedra of the two potassium atoms are constituted of four oxygen atoms from four different oxalate groups (common to CdO_8 and ZrO_8 polyhedra) and four oxygen atoms from water molecules. The oxalate groups act here as monodentate ligands, whereas they are bidentate with respect to the zirconium and cadmium atoms. The discrepancies within the group of distances *g* show the high distortion level of the potassium coordination dodecahedra. It can be noted that the distance between two oxygen atoms from water molecules (*b*) is much larger than that between the oxygen atoms of the oxalate group (*a*), which explains the distortion.

There is only one oxalate group in the asymmetric unit, which is nearly planar with a standard mean deviation from planarity of less than 0.02 Å. The oxalate groups lie perpendicular to each other due to the 4 axis of the structure.

Table 3 Bond distances (Å) and angles (°) with their standard deviations for $CdZrK_2(C_2O_4)_4 \cdot 8H_2O$

Within the CdO_8 polyhedra			
M–A		**M–B**	
Cd–O2, O2$^{\mathrm{iv,v,vi}}$	2.499(2)	Cd–O3$^{\mathrm{iv,vii,viii}}$	2.338(2)
a		***b***	
O2–O2$^{\mathrm{iv}}$	2.747(3)	O3–O3$^{\mathrm{v,vi}}$	3.376(2)
O2$^{\mathrm{v}}$–O2$^{\mathrm{vi}}$	2.747(3)	O3$^{\mathrm{iv}}$–O3$^{\mathrm{v,vi}}$	3.376(2)
m		***g***	
O2–O3	2.732(2)	O2–O3$^{\mathrm{v}}$	3.010(4)
O2$^{\mathrm{iv}}$–O3$^{\mathrm{iv}}$	2.732(2)	O2–O3$^{\mathrm{vi}}$	3.219(2)
O2$^{\mathrm{v}}$–O3$^{\mathrm{v}}$	2.732(2)	O2$^{\mathrm{iv}}$–O3$^{\mathrm{v}}$	3.219(2)
O2$^{\mathrm{vi}}$–O3$^{\mathrm{vi}}$	2.732(2)	O2$^{\mathrm{iv}}$–O3$^{\mathrm{vi}}$	3.010(4)
		O2$^{\mathrm{v}}$–O3	3.010(4)
		O2$^{\mathrm{v}}$–O3$^{\mathrm{iv}}$	3.219(2)
		O2$^{\mathrm{vi}}$–O3	3.219(2)
		O2$^{\mathrm{vi}}$–O3$^{\mathrm{iv}}$	3.010(4)
Within the ZrO_8 polyhedra			
M–A		**M–B**	
Zr–O4, O4$^{\mathrm{i,ii,iii}}$	2.244(2)	Zr–O1, O1$^{\mathrm{i,ii,iii}}$	2.177(1)
a		***b***	
O4–O4$^{\mathrm{i}}$	2.495(3)	O1–O1$^{\mathrm{ii,iii}}$	3.174(2)
O4$^{\mathrm{ii}}$–O4$^{\mathrm{iii}}$	2.495(3)	O1$^{\mathrm{i}}$–O1$^{\mathrm{ii,iii}}$	3.174(2)
m		***g***	
O1–O4	2.561(2)	O1–O4$^{\mathrm{ii}}$	2.837(2)
O1$^{\mathrm{i}}$–O4$^{\mathrm{i}}$	2.561(2)	O1–O4$^{\mathrm{iii}}$	2.726(2)
O1$^{\mathrm{ii}}$–O4$^{\mathrm{ii}}$	2.561(2)	O1$^{\mathrm{i}}$–O4$^{\mathrm{ii}}$	2.726(2)
O1$^{\mathrm{iii}}$–O4$^{\mathrm{iii}}$	2.561(2)	O1$^{\mathrm{i}}$–O4$^{\mathrm{iii}}$	2.837(2)
		O1$^{\mathrm{ii}}$–O4	2.726(2)
		O1$^{\mathrm{ii}}$–O4$^{\mathrm{i}}$	2.837(2)
		O1$^{\mathrm{iii}}$–O4	2.837(2)
		O1$^{\mathrm{iii}}$–O4$^{\mathrm{i}}$	2.726(2)
Within the $K1O_8$ polyhedra			
M–A		**M–B**	
K1–O2, O2$^{\mathrm{iv,vii,viii}}$	2.756(2)	K1–Ow1, Ow1$^{\mathrm{iv,vii,viii}}$	2.887(2)
A		***b***	
O2–O2$^{\mathrm{iv}}$	2.747(3)	Ow1–Ow1$^{\mathrm{vii,viii}}$	4.118(3)
O2$^{\mathrm{vii}}$–O2$^{\mathrm{viii}}$	2.747(3)	Ow1$^{\mathrm{iv}}$–Ow1$^{\mathrm{vii,viii}}$	4.118(3)
M		***g***	
Ow1–O2$^{\mathrm{vii}}$	3.300(3)	Ow1–O2	3.204(2)
Ow1$^{\mathrm{iv}}$–O2$^{\mathrm{viii}}$	3.300(3)	Ow1–O2$^{\mathrm{iv}}$	4.239(3)
Ow1$^{\mathrm{vii}}$–O2$^{\mathrm{iv}}$	3.300(3)	Ow1$^{\mathrm{iv}}$–O2	4.239(3)
Ow1$^{\mathrm{viii}}$–O2	3.300(3)	Ow1$^{\mathrm{iv}}$–O2$^{\mathrm{iv}}$	3.204(2)
		Ow1$^{\mathrm{vii}}$–O2$^{\mathrm{vii}}$	3.204(2)
		Ow1$^{\mathrm{vii}}$–O2$^{\mathrm{viii}}$	4.239(3)
		Ow1$^{\mathrm{viii}}$–O2$^{\mathrm{vii}}$	4.239(3)
		Ow1$^{\mathrm{viii}}$–O2$^{\mathrm{viii}}$	3.204(2)
Within the $K2O_8$ polyhedra			
M–A		**M–B**	
K2–O4$^{\mathrm{ii,iii,ix,x}}$	2.895(2)	K2–Ow2$^{\mathrm{viii,xi,xii,xiii}}$	2.832(2)
a		***b***	
O4$^{\mathrm{ix}}$–O4$^{\mathrm{x}}$	2.495(3)	Ow2$^{\mathrm{xii}}$–Ow2$^{\mathrm{viii,xiii}}$	4.041(3)
O4$^{\mathrm{ii}}$–O4$^{\mathrm{iii}}$	2.495(3)	Ow2$^{\mathrm{xi}}$–Ow2$^{\mathrm{viii,xiii}}$	4.041(3)
m		***g***	
O4$^{\mathrm{ix}}$–Ow2$^{\mathrm{xii}}$	3.527(3)	O4$^{\mathrm{ix}}$–Ow2$^{\mathrm{viii}}$	4.261(3)
O4$^{\mathrm{x}}$–Ow2$^{\mathrm{xi}}$	3.527(3)	O4$^{\mathrm{ix}}$–Ow2$^{\mathrm{xiii}}$	3.272(2)
O4$^{\mathrm{iii}}$–Ow2$^{\mathrm{viii}}$	3.527(3)	O4$^{\mathrm{x}}$–Ow2$^{\mathrm{viii}}$	3.272(2)
O4$^{\mathrm{ii}}$–Ow2$^{\mathrm{xiii}}$	3.527(3)	O4$^{\mathrm{x}}$–Ow2$^{\mathrm{xiii}}$	4.261(3)
		O4$^{\mathrm{iii}}$–Ow2$^{\mathrm{xi}}$	4.261(3)
		O4$^{\mathrm{iii}}$–Ow2$^{\mathrm{xii}}$	3.272(2)
		O4$^{\mathrm{ii}}$–Ow2$^{\mathrm{xi}}$	3.272(2)
		O4$^{\mathrm{ii}}$–Ow2$^{\mathrm{xii}}$	4.261(3)
Within the oxalate moiety			
C1–C2	1.532(2)	O1–C1–O2	127.1(2)
C1–O1	1.286(2)	O3–C2–O4	127.0(2)
C1–O2	1.223(2)	C1–C2–O3	119.1(1)
C2–O3	1.239(3)	C1–C2–O4	114.0(1)
C2–O4	1.267(2)	C2–C1–O1	113.6(1)
		C2–C1–O2	119.3(1)
Within the water molecules			
Ow1–H11	0.86(3)	H11–Ow1–H12	106(3)
Ow1–H12	0.80(2)	H21–Ow2–H22	109(3)
Ow2–H21	0.85(3)		
Ow2–H22	0.89(3)		

Symmetry codes :(i) $1-x$, $2-y$, z; (ii) $3/2-y$, $1/2+x$, $1/2-z$; (iii) $-1/2+y$, $3/2-x$, $1/2-z$; (iv) $1-x$, $1-y$, z; (v) $1-y$, x, $1-z$; (vi) y, $1-x$, $1-z$; (vii) y, $1-x$, $-z$; (viii) $1-y$, x, $-z$; (ix) $1-x$, $2-y$, $-1+z$; (x) x, y, $-1+z$; (xi) $3/2-x$, $3/2-y$, $-1/2+z$; (xii) $-1/2+x$, $1/2+y$, $-1/2+z$; (xiii) y, $2-x$, $-z$.

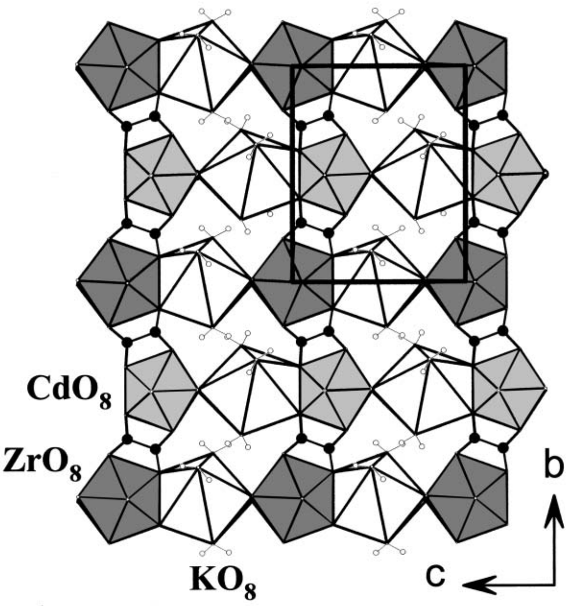

Fig. 2 Partial view of the structure of $CdZrK_2(C_2O_4)_4·8H_2O$ along the *a* axis showing the $(–Cd–ox–Zr–ox–)_\infty$ zigzag chains linked by edge-sharing KO_8 polyhedra. Light grey polyhedra: CdO_8; dark grey polyhedra: ZrO_8; white polyhedra: KO_8; small black circle: C; small white circle: H.

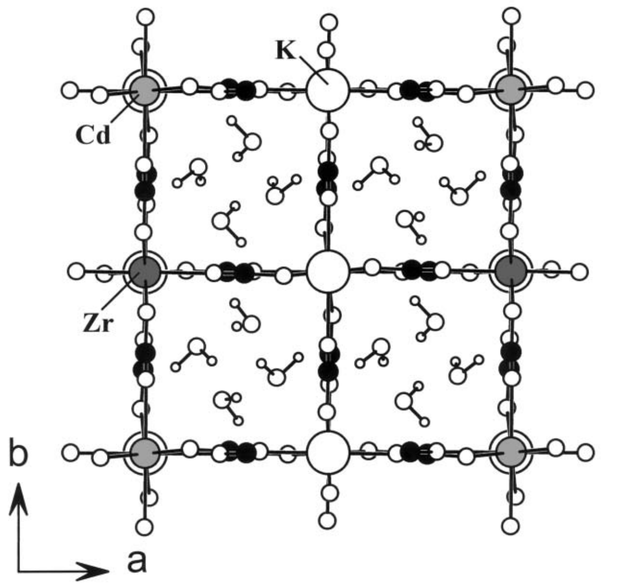

Fig. 3 Projection of the structure of $CdZrK_2(C_2O_4)_4·8H_2O$ along [001]. Large light grey circle: Cd; large dark grey circle: Zr; large white circle: K; small black circle: C; medium white circle: O; small white circle: H.

Within the oxalate group, the various bond lengths and angles [mean bond length: C–C 1.532(2), C–O 1.254(4) Å; mean angles: O–C–O 127(1), C–C–O 116(1)°] are in good agreement with the expected values, reported by Hahn for oxalate compounds.[28]

The water molecules have H–O–H angles of 107.5° and mean O–H distances of 0.85 Å, which is what is expected for X-ray diffraction studies. It can be noted that all water molecules found in the structure belong to the coordination polyhedra of the potassium atoms.

Thermal behaviour

The thermal decomposition of the ternary compound was studied from TG measurements (Fig. 5) and TDXD (Fig. 6), from room temperature to 600 °C under airflow. The chemical formula deduced from the TG curve is $CdZrK_2(C_2O_4)_4·8.5H_2O$. The difference in the water molecules content between the TG analysis and the crystal structure solution is usual with this kind of material with a water molecule content sensitive to water vapour pressure[6,8] and can be explained by the presence of adsorbed water molecules on the surface of the solid. The decomposition of $CdZrK_2(C_2O_4)_4·8.5H_2O$ can be described as a three-step process. The precursor is stable until ~50 °C, where the material starts losing weight and undergoes an important structural change. Indeed, the TDXD plot shows that a new crystalline phase is formed at ~40°C and is stable up to ~85 °C. According to the TG analysis, this intermediate phase would correspond to the tetrahydrated compound with a measured weight loss of 12.0% (theoretical 10.2%). Then, between ~90 and ~115 °C, another structural change is observed in the TDXD plot, which coincides with a second weight loss in the TG curve. This measured weight loss 19.4% agrees well with the departure of the last four water molecules (theoretical 18.5%). The anhydrous phase is stable until ~320 °C and, then, the oxalate entities decompose between ~320 and ~440 °C. Finally diffraction lines of nanocrystalline cubic CdO and tetragonal ZrO_2 appear around 300 °C. The

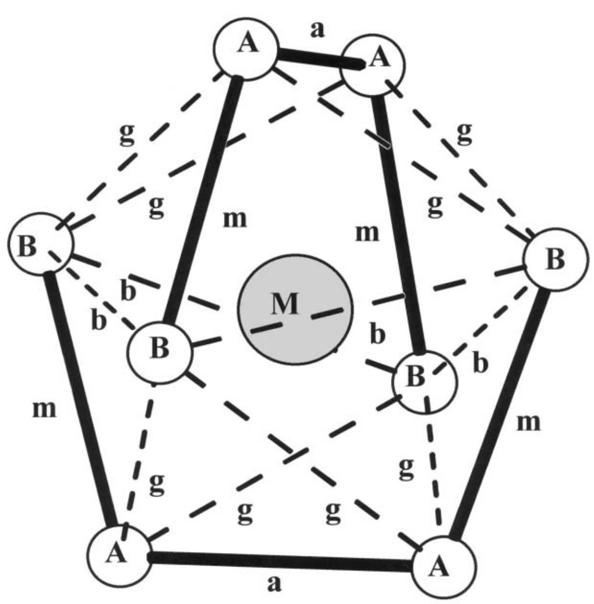

Fig. 4 Representation of the cadmium and zirconium coordination polyhedron. The O–O distances are indicated according to the common notation used by Hoard and Silverton.[12]

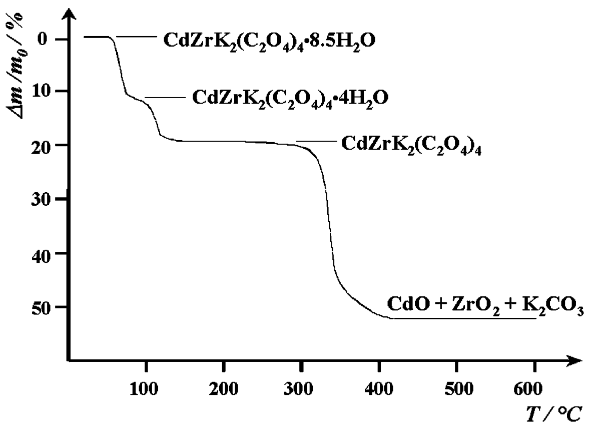

Fig. 5 TG curve for $CdZrK_2(C_2O_4)_4·8H_2O$ under flowing air (5 °C h^{-1}).

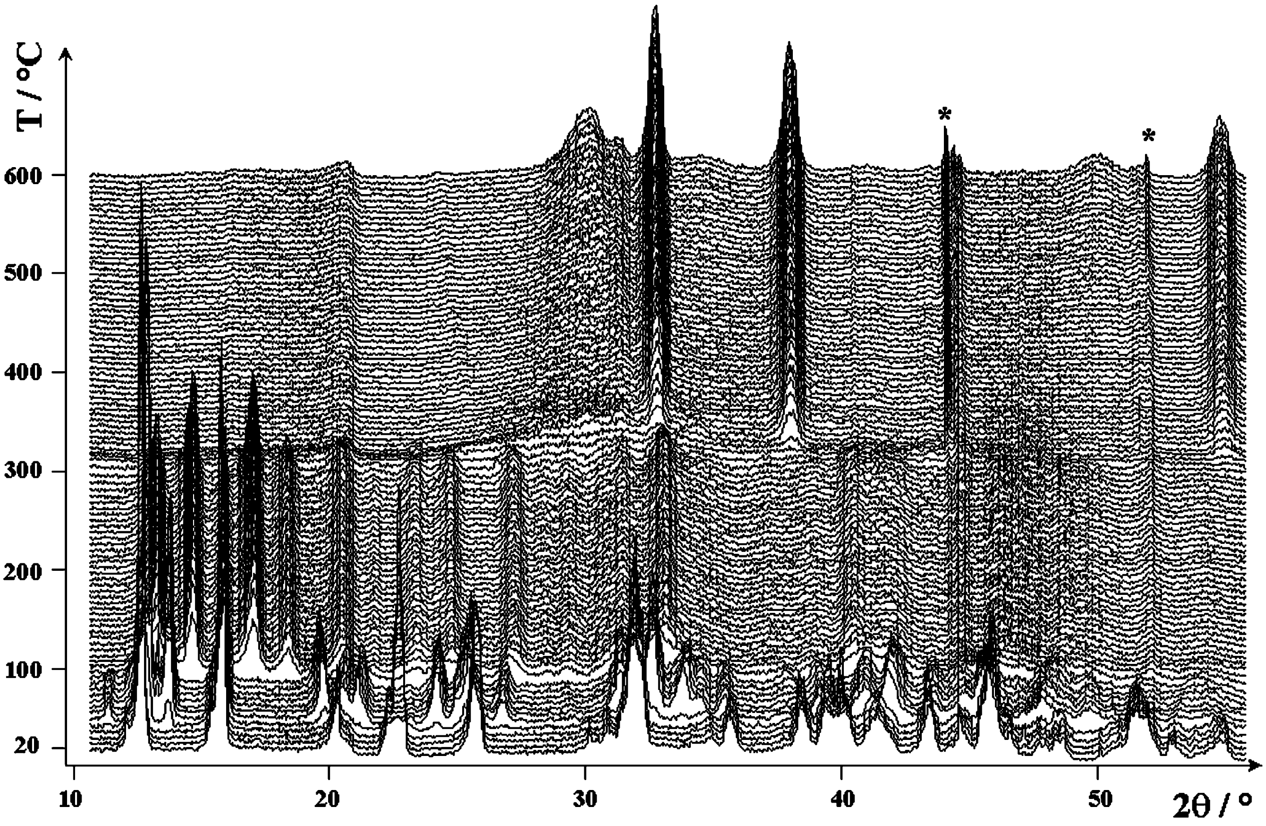

Fig. 6 TDXD plot for $CdZrK_2(C_2O_4)_4{\cdot}8H_2O$ under flowing air (heating rate: 5 °C h^{-1}, counting time: 4200 s $pattern^{-1}$). * spurious diffraction lines due to the sample holder.

lines are particularly broad for ZrO_2, which is in accordance with many studies in which the oxide is crystallised from an amorphous state.[29–31] However, the total weight loss in the TG curve can be explained from the formation of a mixture of CdO, ZrO_2 and K_2CO_3 with an observed weight loss of 52.4% (theoretical 50.4%). Since the TDXD plot does not show any diffraction lines corresponding to potassium carbonate, it can be supposed that it is formed in an amorphous state. Such a feature has already been observed in the thermal decomposition of oxalate-based alkali metals, *e.g.* $La(H_2O)_2K(C_2O_4)_2.H_2O$[32] and $Y(H_2O)Cs(C_2O_4)_2$.[33]

A powder diffraction pattern of the first intermediate phase, $CdZrK_2(C_2O_4)_4{\cdot}4H_2O$, was recorded *in situ* under static air at 35 °C. It was indexed successfully with a monoclinic solution: $a = 8.246(2)$, $b = 15.497(5)$, $c = 9.439(2)$ Å, $\beta = 121.78(1)°$ [$M_{20} = 31$, $F_{20} = 57(0.006, 59)$]. Two possible space groups with the same extinction rules (*C*2/*c* and *Cc*) were retained. The powder data have been submitted to the ICDD[34] for possible inclusion in the Powder Diffraction File. This result indicates that the compound is chemically pure. Attempts to solve *ab initio* the structure were unsuccessful due to the low crystallinity of the product.

Relationships with open-framework structures based on mixed CdO_8 and ZrO_8 polyhedra

An interesting feature of organic–inorganic compounds built from MO_8 polyhedra and oxalate anions is the fact that they display three-dimensional open frameworks. Indeed, the crystal structures of recently prepared new compounds $Cd_2Zr(C_2O_4)_4{\cdot}6H_2O$ (**I**),[6] $CdZr(NH_4)_2(C_2O_4)_4{\cdot}4H_2O$ (**II**) and $CdZr(C_2N_2H_{10})(C_2O_4)_4{\cdot}4H_2O$ (**III**)[9] show 3D arrangements of eight-fold coordinated cadmium and zirconium atoms linked through bidentate oxalate groups. Two types of polyhedra are found in the two different kinds of structures, namely dodecahedra (**I**) and square-based antiprisms (**II** and **III**). The interconnection between the dodecahedra or the antiprisms through oxalate groups leads to two types of structures. Indeed, a dodecahedron exhibits four *m* edges belonging to two perpendicular trapezoids, which allows the connection between MO_8 polyhedra along two directions (Fig. 4). Each *m* edge is spanned by a bichelating oxalate group. Indeed, the lengths of these *m* edges correspond to the distance between two oxygen atoms in an oxalate group. The two *m* edges belonging to the same trapezoid make an angle of about 44° with respect to each other, leading to the formation of a net of perpendicular zigzag chains with a $(\text{–Cd–oxalate–Zr–oxalate–})_n$ sequence as shown in Fig. 7(b) and 8. The other possible eight-fold coordination polyhedron is the square-based antiprism, which is found in compounds **II** and **III**. All CdO_8 and ZrO_8 polyhedra found in these structures have a square antiprismatic configuration with a tilt angle of 60° between the two square bases (Fig. 7(a)). The oxalate groups span two opposite edges of each square base. Thus, two oxalate groups belonging to different square bases make an angle of 60° with respect to each other. This feature leads to the formation of helical chains exhibiting the same sequence as the zigzag ones. Six antiprisms together with six oxalate groups are needed to complete a whole turn of the helix (Fig. 7(a)). It can be noted that each antiprism belongs to two chains. The structures exhibiting this type of polyhedra are thus constituted of a net of interconnected helical chains, which displays tunnels along different directions, as found in phases **II** and **III**.

The two different arrangements described above lead to two chemically identical $[CdZr(C_2O_4)_4]^{2-}$ anionic frameworks with different topologies. Moreover, both topologies display channels along different crystallographic directions where counter-cations of varied sizes and shapes can lie. The helices

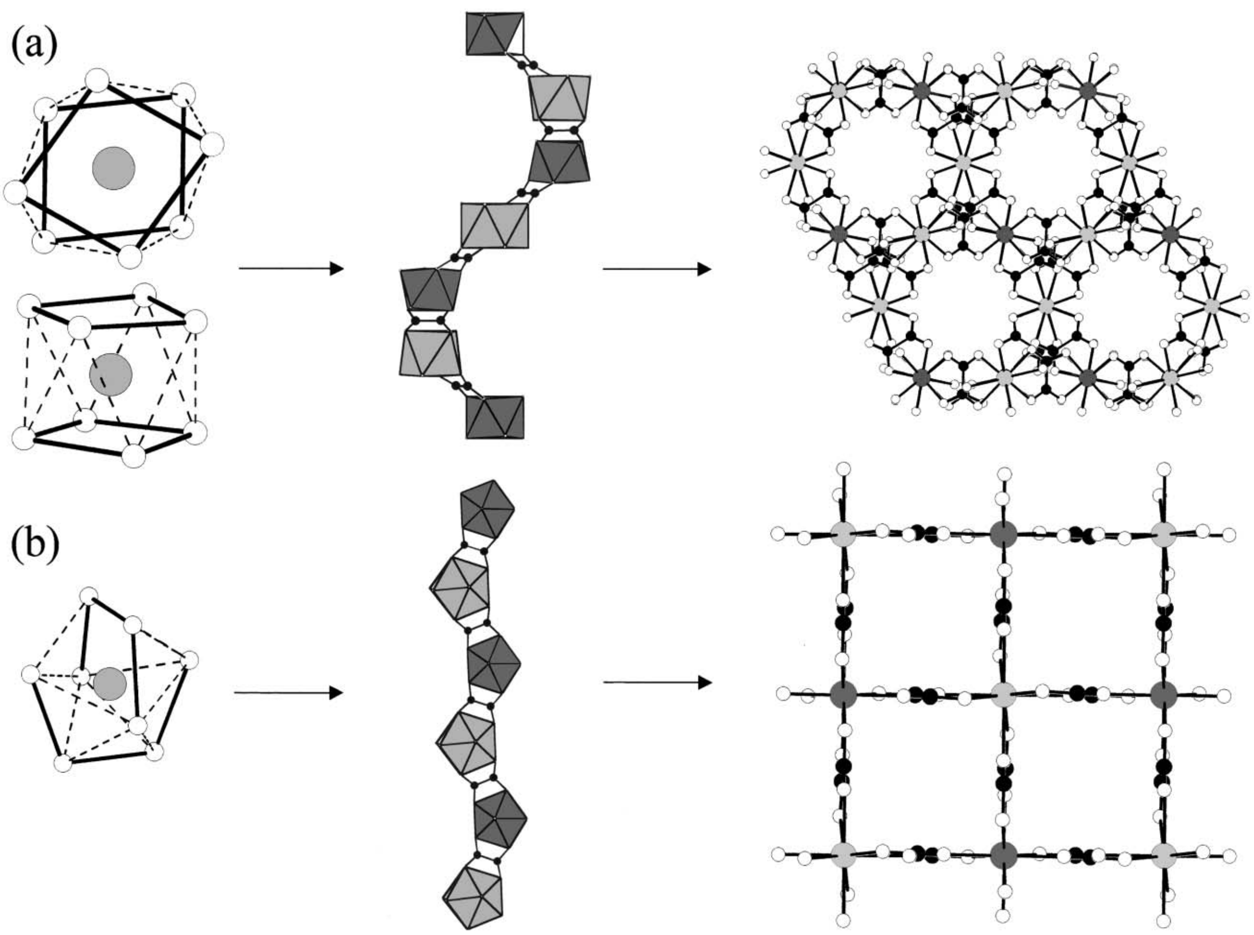

Fig. 7 From MO_8 (M = Cd, Zr) building units to three-dimensional $[CdZr(C_2O_4)_4]^{2-}$ anionic open-frameworks. From left to right: (a) square-based antiprisms with a 60° tilt angle, $(\text{–Cd–ox–Zr–ox–})_\infty$ helical chain, hexagonal anionic framework; (b) dodecahedron, $(\text{–Cd–ox–Zr–ox–})_\infty$ zigzag chain, tetragonal anionic framework.

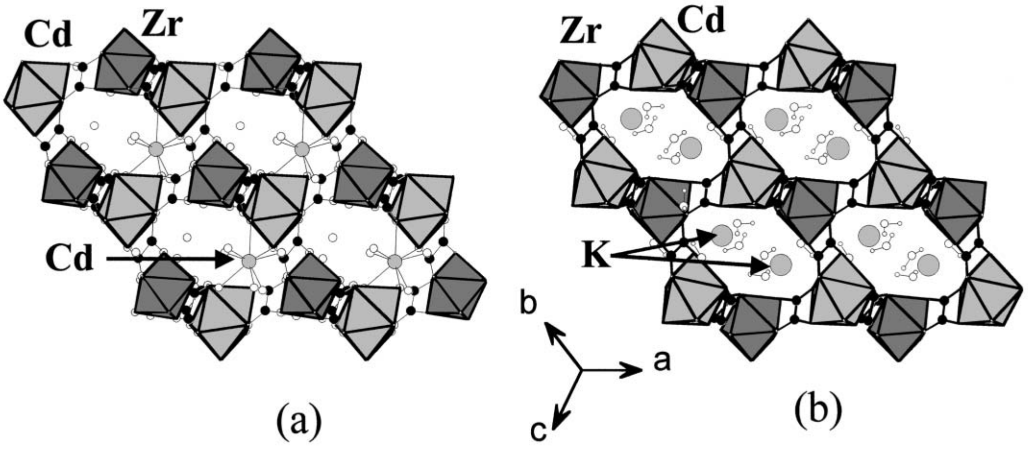

Fig. 8 Projection along [111] of the structures of (a) $Cd_2Zr(C_2O_4)_4{\cdot}6H_2O$ and (b) $CdZrK_2(C_2O_4)_4{\cdot}8H_2O$. The polyhedral network corresponds to the $[CdZr(C_2O_4)_4]^{2-}$ framework.

based structure was obtained with two protonated amines exhibiting different charges: ammonium ion and diprotonated ethylenediamine. In both cases the entities lie in the tunnels along the *c* axis. In one case the anionic charge is balanced by $2[NH_4]^+$ ions and in the other by $[C_2N_2H_{10}]^{2+}$. The zigzag chains based structure was obtained by counter balancing the anionic framework with a divalent metal Cd^{2+} or two monovalent cation K^+, as reported in this study. It is interesting to note that because of the voids present in the anionic skeleton, the electro-neutrality of the compound can be achieved with a relative flexibility. Indeed, in $Cd_2Zr(C_2O_4)_4{\cdot}6H_2O$ one cadmium atom is inserted between two cadmium atoms of the framework described above (Fig. 8(a)). The resulting structure still exhibits channels where water molecules with zeolitic properties are found. On the contrary, in the compound $CdZrK_2(C_2O_4)_4{\cdot}8H_2O$, twice as many atoms of potassium must be inserted to achieve charge balance. One of the potassium atoms replaces the Cd atom and the second is placed in the remaining voids (Fig. 8(b)). As a consequence, no channel is observed in the structure of $CdZrK_2(C_2O_4)_4 \cdot 8H_2O$ and the zeolitic properties of the water molecules are lost because they enter the potassium coordination polyhedra.

To conclude, the chemical combination of eight-fold coordinated atoms offers a variety of possible structure configurations, from which the formation of new compounds can be anticipated. This is demonstrated in the cadmium zirconium family by the existence of two chemically equivalent anionic frameworks, involving varied combinations with different cations. The presence of weakly bonded molecules can also be anticipated from the crystal structure type. Furthermore, substitutions of the cations located in the tunnels of the helical structures or connecting zigzag chains, as reported here for the potassium compound, can be expected.

Acknowledgement

Dr T. Roisnel and Mr G. Marsolier are acknowledged for their technical assistance in single-crystal and powder diffraction data collection.

References

1 A. K. Cheetham, G. Férey and T. Loiseau, *Angew. Chem., Int. Ed.*, 1999, **38**, 3268.

2 C. N. R. Rao, S. Natarajan, A. Choudhury, S. Neeraj and R. Vaidhyanathan, *Acta Crystallogr.*, 2001, **B57**, 1.

3 M. Eddaoudi, D. B. Moler, H. Li, B. Chen, T. M. Reineke, M. O'Keefe and O. M. Yaghi, *Acc. Chem. Res.*, 2001, **34**, 319.

4 D. Trollet, S. Roméro, A. Mosset and J.-C. Trombe, *C. R. Acad. Sci. Paris*, 1997, **325**, 663.

5 T. Bataille, J.-P. Auffrédic and D. Louër, *Chem. Mater.*, 1999, **11**, 1559.

6 E. Jeanneau, N. Audebrand, J.-P. Auffrédic and D. Louër, *J. Mater. Chem.*, 2001, **11**, 2545.

7 M. Louër, D. Louër, F. J. Gotor and J. M. Criado, *J. Solid State Chem.*, 1991, **92**, 565.

8 C. Boudaren, J. P. Auffrédic, M. Louër and D. Louër, *Chem. Mater.*, 2000, **12**, 2324.

9 E. Jeanneau, N. Audebrand and D. Louër, *Chem. Mater.*, 2002, **14**, 1187–1194.

10 B. Matkovic, B. Ribar and B. Zelenko, *Acta Crystallogr.*, 1966, **21**, 719.

11 R. Vaidhyanathan, S. Natarajan and C. N. R. Rao, *J. Solid State Chem.*, 2001, **162**, 150.

12 J. L. Hoard and J. V. Silverton, *Inorg. Chem.*, 1963, **2**, 235.

13 P. Bénard-Rocherullé, J. Rius and D. Louër, *J. Solid State Chem.*, 1997, **128**, 295.

14 D. Louër and J. I. Langford, *J. Appl. Crystallogr.*, 1988, **21**, 430.

15 A. Boultif and D. Louër, *J. Appl. Crystallogr.*, 1991, **24**, 987.

16 J. Rodriguez-Carvajal, in *Collected Abstracts of Powder Diffraction Meeting*, Toulouse, France, 1990, pp. 127–128.

17 T. Roisnel and J. Rodriguez-Carvajal, *Mater. Sci. Forum*, 2001, **118**, 378.

18 J. Plévert, J. P. Auffrédic, M. Louër and D. Louër, *J. Mater. Sci.*, 1989, **24**, 1913.

19 Nonius, Kappa CCD Program Software, Nonius BV, Delft, The Netherlands, 1998.

20 Z. Otwinowski and W. Minor, *Methods Enzymol.*, 1997, **276**, 307.

21 P. Coppens, *Crystallographic Computing*, ed. F. R. Ahmed, S. R. Hall and C. P. Huber, Munksgaard Publishers, Copenhagen, 1970, pp. 255–270.

22 K. Brandenburg and M. Berndt, Diamond (version 2.1e), Crystal Impact, Bonn, 2001.

23 A. Altomare, M. C. Burla, M. Camalli, G. Cascarano, C. Giacovazzo, A. Guagliardi, A. G. G. Moliterni, G. Polidori and R. Spagna, *J. Appl. Crystallogr.*, 1999, **32**, 115.

24 G. M. Sheldrick, SHELXL-97: Programs for Crystal Structure Refinement, University of Göttingen, Göttingen, 1997.

25 M. Nardelli, *J. Appl. Crystallogr.*, 1999, **32**, 563.

26 L. J. Farrugia, *J. Appl. Crystallogr.*, 1999, **32**, 837.

27 I. D. Brown, *J. Appl. Crystallogr.*, 1996, **29**, 479.

28 T. Hahn, *Z. Kristallogr.*, 1957, **109**, 438.

29 G. T. Mamott, P. Barnes, S. E. Tarling, S. L. Jones and C. J. Norman, *Powder Diffr.*, 1988, **3**, 234.

30 P. Bénard, J. P. Auffrédic and D. Louër, *Powder Diffr.*, 1993, **8**, 39.

31 R. Srinivasan, C. R. Hubbard, O. B. Cavin and B. H. Davis, *Chem. Mater.*, 1993, **5**, 21.

32 T. Bataille, M. Louër, J.-P. Auffrédic and D. Louër, *J. Solid State Chem.*, 2000, **150**, 81.

33 T. Bataille, J.-P. Auffrédic and D. Louër, *J. Mater. Chem.*, 2000, **10**, 1707.

34 International Centre for Diffraction Data, Newtown Square, PA.